Compton Scattering Effects on the Spectral and Temporal Properties of Terrestrial Gamma-Ray Flashes

Wei Xu, Sebastien Celestin, Victor P. Pasko, Robert A. Marshall

JGR Space Physics

RESEARCH ARTICLE
10.1029/2019JA026941

Compton Scattering Effects on the Spectral and Temporal Properties of Terrestrial Gamma-Ray Flashes

Wei Xu[1], **Sebastien Celestin**[2], **Victor P. Pasko**[3], **and Robert A. Marshall**[1]

[1]Department of Aerospace Engineering Sciences, University of Colorado Boulder, Boulder, CO, USA, [2]LPC2E, University of Orleans, CNRS, Orleans, France, [3]Communications and Space Sciences Laboratory, Department of Electrical Engineering, Pennsylvania State University, University Park, PA, USA

Key Points:
- We quantify the Compton scattering effects in terms of temporal dispersion and energy spectra produced by tilted TGF geometry
- Offset distance between lightning source and satellite cannot be used as a single parameter characterizing Compton scattering effects
- We show that Fermi-measured TGF pulses, including the asymmetric ones with longer rise time, are consistent with Compton scattering effect

Correspondence to:
Wei Xu,
Wei-Xu@colorado.edu

Citation:
Xu, W., Celestin, S., Pasko, V. P., & Marshall, R. A. (2019). Compton scattering effects on the spectral and temporal properties of terrestrial gamma-ray flashes. *Journal of Geophysical Research: Space Physics*, *124*, 7220–7230. https://doi.org/10.1029/2019JA026941

Received 13 MAY 2019
Accepted 29 JUL 2019
Accepted article online 7 AUG 2019
Published online 17 AUG 2019

Abstract Terrestrial gamma-ray flashes (TGFs) are high-energy photon bursts originating from the Earth's atmosphere. In this study, using first-principles Monte Carlo simulations, we quantify the effects of Compton scattering on the temporal and spectral properties of TGFs induced by a tilted source geometry. Modeling results indicate that the source orientation is a critical parameter in TGF analysis but has been significantly underestimated in previous studies. Offset distance between the lightning source and satellite location cannot be used as a single parameter characterizing Compton scattering effects. In the tilted geometry, Compton scattering effects are more pronounced in the falling part of TGF pulses and can lead to an increase of the falling part of TGF pulses by several tens of microseconds. Moreover, by performing curve-fitting analysis on simulated TGF light curves, we explain how the symmetric and asymmetric pulses measured by the Gamma-Ray Burst Monitor on Fermi satellite are consistent with the Compton scattering effects. Fermi-measured TGF pulses can be fully explained using Gaussian-distributed TGF sources with an average duration of ~206 μs.

1. Introduction

Terrestrial gamma-ray flashes (TGFs), first detected in 1994 by the Burst and Transient Source Experiment (BATSE) instrument aboard the Compton Gamma-Ray Observatory (Fishman et al., 1994), are high-energy photon bursts produced in close association with lightning activity in the Earth's atmosphere. This phenomenon has been abundantly observed by low-Earth-orbit satellites, including the Reuven Ramaty High Energy Solar Spectroscopic Imager (RHESSI) (Smith et al., 2005), the Fermi Gamma-ray Space Telescope (Briggs et al., 2010), and the Astrorivelatore Gamma a Immagini Leggero satellite (Marisaldi et al., 2010).

Space-borne measurements of energy spectra have been widely used to uncover the acceleration mechanism of TGFs (e.g., Dwyer et al., 2012). Dwyer and Smith (2005) first demonstrated that the mechanism of relativistic runaway electron avalanches (RREAs) can reproduce the cumulative TGF spectra measured by RHESSI. The mechanism of relativistic feedback from positrons and X-rays (Dwyer, 2008, 2012) has been further proposed since extensive air showers solely cannot provide sufficient number of seed electrons for RREA processes to explain the observed TGF fluences. On the other hand, Celestin and Pasko (2011) have suggested theoretically that the production of thermal runaway electrons by streamer discharges during the negative corona flash stage of stepping lightning leaders (Moss et al., 2006) could explain TGFs. Based on this mechanism, modeling studies have shown that the energy spectra of bremsstrahlung photons resulting from thermal runaway electrons produced by high-potential lightning leaders are consistent with satellite measurements (Xu et al., 2012).

Space-borne measurements of light curves have been long used to constrain the source properties of TGFs (e.g., Connaughton et al., 2010; Fitzpatrick et al., 2014; Grefenstette et al., 2008, 2010; Nemiroff et al., 1997). More recently, Fishman et al. (2011) have thoroughly examined the temporal properties of TGFs as observed by the Gamma-Ray Burst Monitor (GBM) on Fermi and revealed that a majority of TGF events have typical durations ranging from 0.1 to 0.4 ms, while pulses as brief as ~50 μs have also been seldomly recorded. The lower threshold for the duration of TGF pulses, as later pointed out by Celestin and Pasko (2012), is consistent with the Compton scattering effects, that is, the temporal dispersion and energy spectral softening due to the increased amount of Compton scattering collisions that photons undergo while traversing through the atmosphere. Furthermore, by analyzing the Fermi-measured pulses using the Norris function (Norris et al.,

1996), Foley et al. (2014) found that 67% of TGF pulses detected are asymmetric with fall time significantly longer than rise time, suggesting that these asymmetric pulses tend to be consistent with the mechanism of relativistic feedback discharges.

Analyses of lightning sferics have narrowed down TGF sources to normal polarity intracloud lightning discharges (+IC; e.g., Lu et al., 2010; Shao et al., 2010; Stanley et al., 2006) and more precisely to the development stage of initial leaders (e.g., Marshall et al., 2013; Lyu & Cummer, 2018). Radio emissions have been widely used to estimate the offset distance from the parent lightning discharge, and those recorded simultaneously with satellite measurements have been suggested to be signatures of relativistic electrons at the TGF source (e.g., Connaughton et al., 2013; Mailyan et al., 2018). More recently, using a low-frequency interferometric lightning mapping array, Lyu et al. (2016) have reconstructed the three-dimensional structure of initial leader steps during IC discharges. Most of the initial leader steps and channels were found to be tilted away from the vertical direction; such tilted geometry could mislead the interpretation of position-dependent TGF observation from space. The importance of tilted source geometry has been repeatedly emphasized in previous studies, for example, by Hazelton et al. (2009) while investigating the dependence of TGF energy spectra on offset distances, by Fitzpatrick et al. (2014) while studying the temporal and spectral evolution of TGFs, and by Mailyan et al. (2016) while performing spectral analysis on individual TGF events measured by Fermi GBM. Marshall et al. (2015) similarly showed the need for a tilted radiating dipole geometry in compact intracloud discharges to explain the signatures of elves in the lower ionosphere.

Despite the increased emphasis, the tilted TGF geometry still remains poorly understood and has not been investigated in detail in previous studies. Critical to the accurate interpretation of satellite measurements is therefore the development of a quantitative understanding on the tilted TGF geometry, and this represents the goal of the present study. Using first-principles Monte Carlo simulations and characteristic TGF sources, we first quantify the increased Compton scattering effects on the temporal and spectral properties of TGFs induced by the tilted source geometry. Moreover, we show how the Compton scattering effects can explain the symmetric and asymmetric pulses measured by Fermi GBM and thereby estimate a characteristic timescale for TGF-producing processes.

2. Model Formulation

In this study, we explore the Compton scattering effects in tilted geometry using characteristic TGF sources and a Monte Carlo scattering and propagation model (Xu et al., 2012, 2014). This model is employed to simulate the photon transport through the Earth's atmosphere and was developed based on the description in Østgaard et al. (2008). Three main collision types for photons with energies between 10 keV and 100 MeV are considered: photoelectric absorption, Compton scattering, and electron-positron pair production. This model has been validated through calculations of TGF energy spectra based on RREA theory and comparisons with previously reported results (e.g., Celestin et al., 2012, 2015; Xu et al., 2012, 2017). Here we introduce the TGF source used in the present study.

The goal of this work is to investigate tilted TGFs, irrespective of the exact production mechanism. Thus, we disregard the possible differences in terms of energy spectra and/or duration predicted by the two main production mechanisms that have so far provided good agreements with satellite measurements (e.g., Dwyer et al., 2012; Xu et al., 2015). For this purpose, the energy spectra that would be produced by bremsstrahlung emission of RREA processes (Dwyer et al., 2012) are used for source photons:

$$f(\varepsilon) \propto \frac{\exp\left(-\varepsilon/\varepsilon_c\right)}{\varepsilon}, \tag{1}$$

where ε is the photon energy, $f(\varepsilon)$ is the energy distribution of source photons, ε_c is the high-energy cutoff of RREA distribution, and a typical value of 7 MeV is adopted for ε_c (e.g., Carlson et al., 2007; Dwyer & Smith, 2005). As for the spatial distribution, source photons are considered to be produced within a sphere with a radius of 1 km (Dwyer et al., 2012) centered at 12 km altitude (e.g., Cummer et al., 2014; Xu et al., 2012). Following previous TGF studies (e.g., Gjesteland et al., 2010; Østgaard et al., 2012), the temporal distribution of source photons is assumed to be Gaussian; the duration of TGF source is chosen to be 80, 150, 400, or 1,000 μs between $\pm 2\sigma$, where σ is the standard deviation; a random number between 0 and the source duration is drawn from the Gaussian distribution and then assigned as the initial production time to

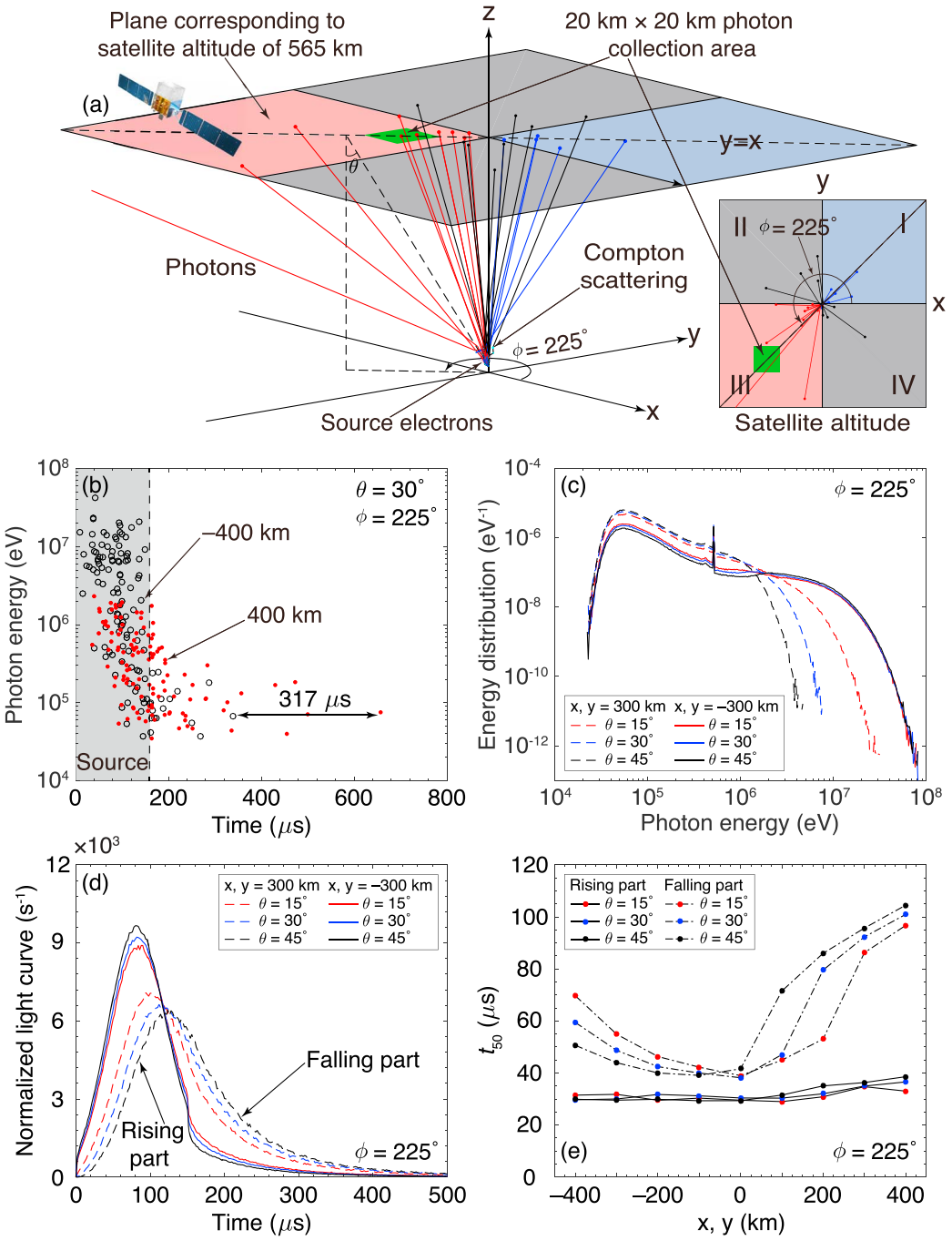

Figure 1. Modeling of tilted TGF geometry. (a) Illustration of the simulation domain used for the modeling of tilted TGF geometry. The inset shows the scatter plot of those bremsstrahlung photons that arrive at satellite altitudes. (b) Energy of those photons measured in two 120-counts TGF events at positions (−400, −400, and 565 km) and (400, 400, and 565 km) versus their time of arrival. (c) Energy spectra and (d) characteristic light curves of those photons recorded at positions (−300, −300, and 565 km) and (300, 300, and 565 km) for different tilt angles (θ = 15°, 30°, and 45°). (e) t_{50} calculated for the rising and falling parts of TGF light curves at different locations (−400 km < x, y < 400 km) for different tilt angles.

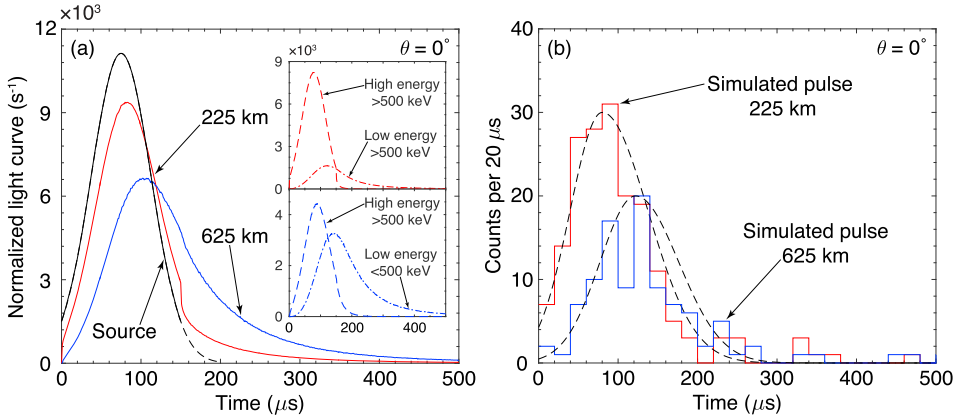

Figure 2. (a) Characteristic TGF pulses that would be measured using ideal detectors at locations inside (225-km offset distance) and outside (625-km offset distance) the source photon beam. The light curves are normalized so that the integration over time yields unity; the duration of TGF source used in this simulation is 150 μs between $\pm 2\sigma$ (solid black curve). The upper and bottom insets show the high-energy (>500 keV) and low-energy (<500 keV) compositions at offset distances of 225 and 625 km, respectively. (b) Examples of Monte-Carlo-simulated TGF pulses at the same offset distances, as well as the corresponding best Norris fits (dashed lines). These results are obtained using the vertical source and broad beam geometry with a half angle of 45°.

each source photon. We have verified that, if a source altitude of 10 km is instead used, the conclusions of this work do not change significantly.

The tilted step of initial leaders is explicitly simulated using two angles: θ and ϕ, similar to those defined in the spherical coordinate system. Specifically, θ is the polar angle of the source photon beam with respect to the zenith direction, and ϕ is the azimuth angle between the $+x$ direction and the orthogonal projection of the beam axis on the xy plane. Defined this way, θ describes the extent of how the source photon beam is tilted away from the zenith direction. Figure 1a is an illustration of the simulation domain used for the modeling of tilted TGF beams. In present simulations, a broad beam geometry is used for source photons; their velocities are assumed to be isotropic within a half angle of 45° from the beam axis (e.g., Carlson et al., 2007; Dwyer & Smith, 2005; Dwyer et al., 2012); this half-angle assumption is utilized in both vertical and tilted simulations. Knowing θ and ϕ, photon velocities can be readily reoriented from the vertical direction, to mimic the bremsstrahlung production by tilted stepping leaders.

Three-dimensional interferometric images have shown that initial leader steps are mostly tilted away from the zenith direction with an angle between 6° and 38° (Lyu et al., 2016). Thus, θ is chosen to be 15°, 30°, or 45° for the simulation of tilted TGF beams. As explained later in the paper, for the comparison with Fermi measurements, vertical source beams, corresponding to the θ value of 0°, are also used. The Compton scattering effects in tilted TGF geometry is primarily determined by the angle θ, and for the sake of simplicity, ϕ is fixed to be 225°. This ϕ value is chosen in order to simulate TGF sources that are tilted toward the third quadrant (see the inset in Figure 1a); in this scenario, gamma rays that arrive at satellite altitudes (565 km) are no longer symmetric with respect to the z axis; such geometry quantifies Compton scattering effects of photons that are recorded at satellite altitude in regions inside (the third quadrant) and outside (the first quadrant) of the source photon beam. In particular, for this comparison, we have utilized 20km × 20km squares along the line of $y = x$ as the photon-collection area at satellite altitudes (see the photon-collection area denoted in Figure 1a). This square photon-collection area is only used in tilted-geometry simulations to quantify the Compton scattering effects (Figure 1), while concentric rings with a width of 1 km between the inner radius and outer radius are used as the photon-collection area only in untilted-geometry simulations when the tilt angle θ is 0° (Figures 2 and 3). This approach is chosen because the system is symmetric with respect to the z axis in this scenario and concentric rings largely shorten the computation time.

We also aim to estimate the production duration of TGFs using the rise and fall time distributions of Fermi-measured TGFs (Foley et al., 2014). For this particular calculation, due to the lack of reliable data on the percentage of tilted TGFs and tilt angles, we opt to simulate TGF light curves as would be produced by vertically propagating sources with four durations (80, 150, 400, and 1,000 μs). Foley et al. (2014) have not considered overlapping or poorly constrained pulses and only analyzed those clearly isolated pulses with

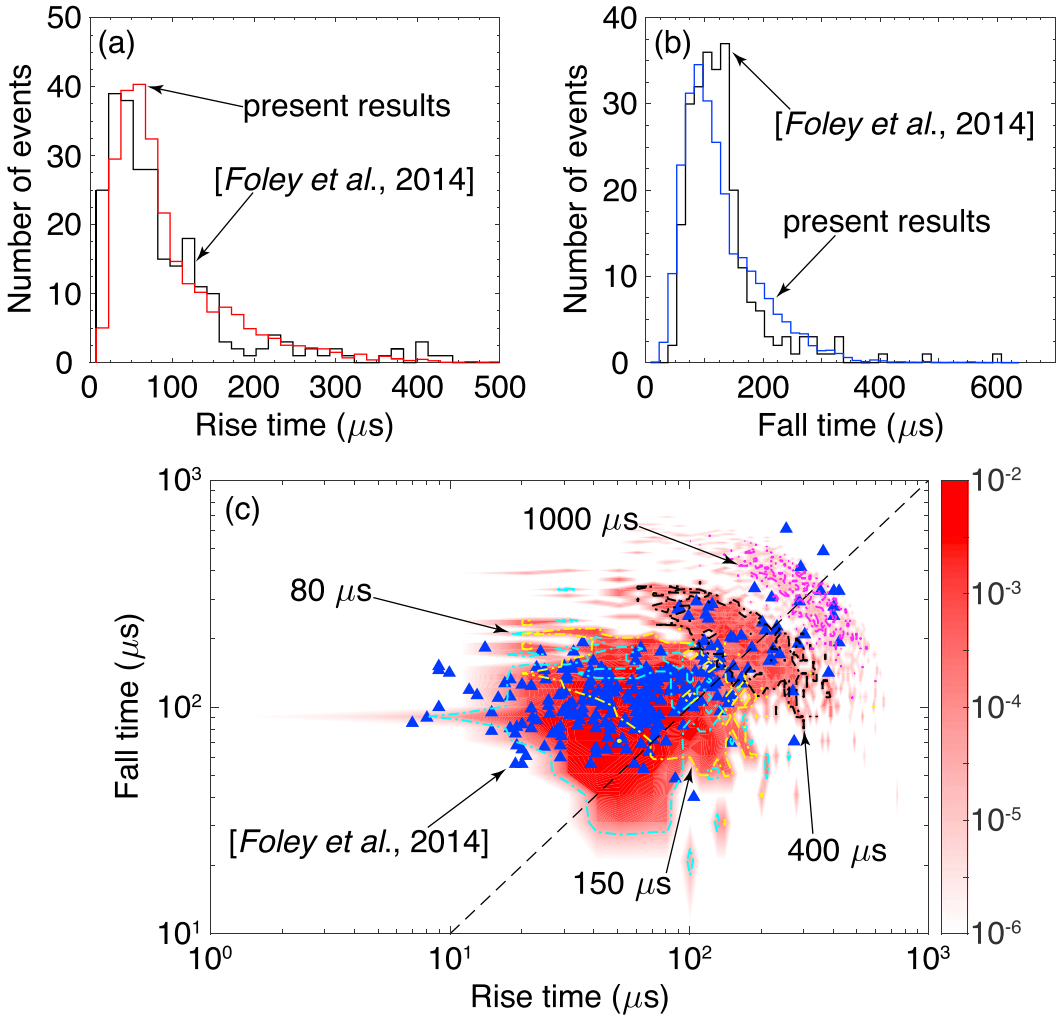

Figure 3. Comparison of (a) rise and (b) fall time distributions between analysis results of Fermi-measured TGF pulses (Foley et al., 2014) and present modeling results. The results show the best fit to the rise and fall time distributions reported in Foley et al. (2014, Figure 5) and are obtained by assuming that the percentage of TGF sources with durations of 80, 150, 400, and 1,000 μs is 25%, 48%, 26%, and 1%, respectively. (c) Comparison of fall time versus rise time between the results reported in Foley et al. (2014, Figure 3) and present modeling results. This distribution represents the probability for measuring a TGF pulse with rise and fall times indicated by the *x* and *y* axes; the dashed contour lines are calculated using the rise and fall times of TGF pulses produced by sources with different durations; they delineate the temporal space caused by different source durations. These results are obtained using the vertical source and broad beam geometry with a half angle of 45°.

single peak and well-constrained parameters. Hence, in this study, 1,000 single-peak clearly isolated pulses are calculated for offset distances up to 800 km away from the lightning discharge and for each source duration, representing 1,000 random TGF events. The number of pulses at different offset distances is chosen accordingly from the offset distance distribution in the first Fermi GBM catalog (Roberts et al., 2018). As for the photon counts in each pulse, we have used the counts as typically recorded by GBM detectors at the corresponding offset distance, as reported in Briggs et al. (2013, Figure 8c). However, this distribution of photon counts versus offset distance was derived using both triggered and off-line search TGFs, while only triggered events have been investigated by Foley et al. (2014). For the purpose of direct comparison, we have rescaled the photon count distribution in Briggs et al. (2013, Figure 8c) so that the average counts per TGF event are the same as triggered events (~100 counts per event; Foley et al., 2014). We emphasize that, even though vertical TGF sources are used for the comparison with Foley et al. (2014), similar pulses can also be obtained in tilted TGF geometry (see Figures 1d and 2a), and thus, the results of rise and fall times would not be substantially altered.

To calculate the light curve at a given offset distance r, we first accumulate all the photons that escape the atmosphere and arrive in the concentric ring defined by $r \pm 1$km (Celestin & Pasko, 2012). Second, a given number of photons are then randomly picked from Monte Carlo simulation results, and as mentioned above, this number is chosen on the basis of Fermi measurements (Briggs et al., 2013, Figure 8c). The time of arrival for each selected photon is further calculated by subtracting the time spent as if the photon were to follow a straight path to the detector (e.g., Celestin & Pasko, 2012; Østgaard et al., 2008). Finally, we calculate the light curve by sampling selected photons using 2-μs bins, that is, the intrinsic time resolution for time-tagged events of Fermi GBM (Briggs et al., 2010). No instrumental effects have been considered in this light curve calculation. However, as will be explained below, these instrumental limitations have been demonstrated to have small influence on the temporal parameters of most TGF pulses (Foley et al., 2014; Tierney et al., 2013).

After obtaining the light curves, we use a Norris fitting procedure (Foley et al., 2014; Norris et al., 1996) to investigate the temporal structure of TGFs. A curve-fitting model is developed based on the description in Foley et al. (2014). Specifically, the Norris function (Norris et al., 1996) is employed to fit the rising and falling parts of pulses separately with three parameters: the maximum emission rate and the rise and fall time constants. The peakedness factor in the Norris function is fixed to be 2 (Foley et al., 2014), which defines a two-sided Gaussian using rise and fall time constants. We use the Poisson maximum likelihood function in order to evaluate the goodness of fit (Briggs et al., 2010; Foley et al., 2014), and the best fit is determined from the set of parameters that maximizes the likelihood function.

We note that simulated TGF pulses may contain a "tail" of photon counts, that is, a sequence of single-count bins due to discrete arrivals of single photon at relatively later time. An example is shown in Figure 2b: the discrete bins in the simulated pulse at the offset distance of 625 km at time greater than ~300 μs. Such tail is caused by the effects of Compton scattering and, thus, not unphysical (see Figure 5 in Fishman et al., 2011) but could bias the Norris fitting toward longer fall times; it is also likely that this tail could be buried within the noise of background radiation. Given that the light curves analyzed by Foley et al. (2014) are clearly isolated emission episodes, the photon counts in the tail of simulated pulses are not considered in the present curve-fitting procedure (see the best fits in Figure 2b).

3. Results

Figure 1 shows modeling results of tilted TGF geometry. The TGF source used in this set of simulations has a duration of 150 μs between $\pm 2\sigma$ (Gjesteland et al., 2010; Østgaard et al., 2012) with three tilt angles: $\theta = 15°$, 30°, and 45°. Figure 1b shows the energy of those photons measured in two 120-counts TGF events at positions (−400, −400, and 565 km) and (400, 400, and 565 km) versus their time of arrival. These two locations have the same offset distance from the TGF source, but one is well inside the source photon beam, whereas the other one is outside. These results are obtained by collecting photons at satellite altitudes in the square regions defined by (−400 ± 10 km, −400 ± 10 km, and 565km) and (400 ± 10 km, 400 ± 10 km, and 565 km), respectively. We have verified that, if a smaller photon-collection area (10km × 10km) is instead used, the results of light curve and energy spectra do not change noticeably while being computationally more expensive because a larger number of photons are required to build up a smooth distribution.

Because the source photon beam is tilted toward $-x$ and $-y$ directions, photons arriving in the region near (−400, −400, and 565 km) are mainly those that are less frequently scattered or even unscattered by the atmosphere, as evident by the population of photons with energies greater than 10 MeV and time of arrival less than 150 μs. In contrast, at the opposite location, photons appear to be much less energetic with significantly later time of arrival. The last photon arrives at ~340 and ~657 μs, and the most energetic photon has an energy of ~41 and ~2.3 MeV for the event measured in the third and first quadrants, respectively. These differences can be attributed to the fact that source photons in the initial beam need to undergo multiple scatterings, and only those that are deflected into the right slant angle can be detected in the nearby region of (400, 400, and 565 km). The energy reduction and temporal dispersion shown in this figure illustrate the maximum effects of Compton scattering.

At the same offset distance, the tilted geometry can lead to distinctively different energy spectra and light curves, as shown in Figures 1c and 1d. Figure 1c shows the energy spectra of those photons measured at positions (−300, −300, and 565 km) and (300, 300, and 565 km) for different tilt angles: $\theta = 15°$, 30°, and 45°. Figure 1d shows the light curves. This offset distance is chosen as it is typical in satellite measurements

(e.g., Briggs et al., 2013). At the position (300, 300, and 565 km), as θ changes from 15° to 45°, the source beam is tilted further away, and the energy distribution becomes considerably softer with the maximum energy decreasing from ~32 to ~4.7 MeV. However, the distributions at the opposite side are fairly similar. The effects of Compton scattering can be roughly assessed using the distance between where the source photon beam is pointed at and where photons are recorded. On average, to reach further distances, photons experience more scatterings by air molecules, deposit more energy in the atmosphere, and the Compton scattering effect is enhanced. This point is also evidenced by the high- and low-energy compositions of TGFs as presented in Figure 2a.

Figure 2a shows modeling results of characteristic TGF light curves that would be measured using ideal detectors at offset distances of 225 and 625 km from the parent lightning discharge. They are normalized so that the integration of each pulse over time yields unity; the source duration is 150 μs; the source photon beam is assumed to be vertical in this calculation ($\theta = 0°$). The sharp drop of the pulse at the offset distance of 225 km around 150 μs is caused by the temporal distribution assumed for the TGF source. The upper and bottom insets show the high-energy (>500 keV) and low-energy (<500 keV) compositions at the offset distances of 225 and 625 km, respectively. One clearly sees that, when the offset distance increases from 225 to 625 km, the pulse becomes considerably wider with the peak shifting from ~83 to ~107 μs and evolves from symmetric into asymmetric. Both the rising and falling parts of the pulse become noticeably flatter with increasing offset distances, corresponding to larger values of rise and fall time constants as defined in Norris fitting. This prolongation of rise and fall times is a consequence of the increased number of low-energy photons that are heavily scattered by the atmosphere, as shown in the insets.

Although calculated using a vertical source, the pulses presented in Figure 2a are more broadly representative of those typically measured inside and outside the source photon beam, even in the tilted geometry, as shown in Figure 1d. The pulses measured at the position (−300, −300, and 565 km) are similar to those measured at the offset distance of 225 km in the untilted case (Figure 2a). With increasing tilt angle, the temporal spread in the light curve measured at the position (300, 300, and 565 km) becomes notably greater. For locations inside the source photon beam, high-energy photons dominate the light curve, whereas the low-energy portion becomes almost comparable at locations outside the source photon beam (see the insets of Figure 2a). Consequently, the pulses measured at the position (−300, −300, and 565 km) are fairly similar to the temporal distribution assumed for the TGF source since it is well preserved by the population of high-energy photons. For the other location, as θ increases, the fraction of low-energy photons becomes larger, and the Compton scattering effect is amplified, giving rise to progressively flatter pulses.

To quantitatively describe the Compton scattering effects on light curves, we have calculated the characteristic timescale using the measure t_{50} as typically used in TGF studies (e.g., Celestin & Pasko, 2012; Fishman et al., 2011). This parameter specifically corresponds to the time interval between 25% and 75% of the arrival of photon counts detected during the event. Figure 1e shows the t_{50} calculated for the rising and falling parts of TGF light curves at different locations ($-400\ \text{km} < x, y < 400\ \text{km}$) for different tilt angles. The Compton scattering effects on the rising part are not as pronounced as those on the falling part, but one sees a variation of t_{50} by approximately 9 μs in the case of a 45° tilt angle. For the falling part, t_{50} is increased by as large as ~58, ~63, and ~66 μs for the tilt angle of 15°, 30°, and 45°, respectively. It is also interesting to observe that the minimum value of the falling part shifts toward $+x$ direction as θ decreases. This feature is roughly in accordance with the change in the position at which the source photon beam is pointed at.

We have also estimated the source duration of TGF-producing processes using Fermi measurements. Figure 2b shows examples of Monte-Carlo-simulated TGF pulses at the offset distances of 225 and 625 km away from the lightning source, as well as the corresponding best Norris fits. Norris fitting was performed on the light curves with 2-μs resolution. Note that these simulated light curves resemble those typically measured by Fermi GBM in terms of general shape and pulse width, such as events 18 and 33 as documented in Fishman et al. (2011, Figure 5).

Figure 3a shows the comparison of rise time distribution between analysis results of Fermi-measured TGF pulses (Foley et al., 2014) and present modeling results. Figure 3b shows the comparison of fall time distribution. These results are calculated by performing Norris fitting on the simulated TGF pulses with four source durations. For each duration, the best-fit rise and fall times obtained for the 1,000 simulated pulses are first sampled using the same time bins as Foley et al. (2014, Figure 5); the distributions of rise and fall times are

then calculated for each duration and normalized so that the integration over time yields unity. Second, we combine the four durations using a function: $F = \sum_{k=1}^{4} c_k f_k$, where F is the combined rise or fall time distribution, index k scans the four durations assumed for TGF source, c_k is a fitting parameter ($\sum_{k=1}^{4} c_k = 1$), and f_k is the rise or fall time distribution produced by the kth source duration. Defined this way, the parameter c_k represents the percentage of TGF sources with a duration indicated by index k. Finally, the least square criterion is used to evaluate the difference between the combined distribution and that of Foley et al. (2014, Figure 5) and to determine one set of c_k that explains both rise and fall time distributions. The median value is approximately 106 and 140 μs for the rise and fall times of simulated TGF pulses, respectively.

Figure 3c shows the comparison of fall time versus rise time with the analysis results of GBM measurements (Foley et al., 2014, Figure 3). These results are calculated similarly as Figures 3a and 3b but sampled using finer time bins. These bins are specifically a total of 1,000 × 1,000 linear numerical cells, covering a temporal spread from 0 to 1 ms in both rise and fall times. Likewise, we first calculate the 2-D (rise, fall) distribution using the best-fit rise and fall times for each source duration. These 2-D distributions are then weighted using the best c_k as obtained in Figures 3a and 3b and summed together. Figure 3c shows this distribution but normalized so that the sum of this 2-D matrix is unity, representing the probability for measuring a TGF pulse with rise and fall times indicated by the x and y axes. The color bar is thus unitless. The dashed contour lines depict the temporal space caused by different source durations.

The rise and fall time distributions of Fermi-measured TGFs can be best explained if the percentage of TGF source with durations of 80, 150, 400, and 1,000 μs is 25%, 48%, 26%, and 1%, respectively. The slight difference at the first time bin of Figures 3a and 3b is due to the limited number of source durations used in this estimation. These best-fit coefficients imply an average duration of ~206 μs for the underlying TGF-producing processes. This duration, as inversely derived from rise and fall times of Fermi measurements, turns out to be consistent with the 250 μs derived from BATSE measurements (Gjesteland et al., 2010), as well as the variation timescale of 50 μs (one standard deviation σ in Gaussian distributions) derived from the hardness ratio of Fermi-measured pulses (Fitzpatrick et al., 2014). In addition, it is clear that the fall time versus rise time (Foley et al., 2014), including both symmetric and asymmetric pulses, can be fully explained using the four durations. TGF sources with a duration of 80 or 150 μs can produce both symmetric and asymmetric pulses (cyan and yellow lines), while pulses originating from the 400 or 1,000 μs source are mostly symmetric (black and purple lines).

4. Discussion

Using an instantaneous TGF source, Celestin and Pasko (2012) have shown that the effects of Compton scattering could result in a temporal dispersion ranging from ~20 to ~80 μs at offset distances between 100 and 500 km. If the source duration is not substantially greater than this dispersion (<150 μs), the decay part of TGF pulses at large offset distances is dominated by Compton-scattered photons. Therefore, asymmetric pulses would be measured when the intrinsic source duration is not comparable to Compton scattering effects, for example, when TGFs originating from a brief acceleration process are observed at locations outside the source photon beam. This point has also been pointed out by Foley et al. (2014). If the source duration is overwhelmingly longer (>400 μs), the temporal dispersion of Compton scattering becomes insignificant, and the fall time is controlled by that of the source. Therefore, symmetric pulses would be measured at offset distances close to the lightning source, alternatively if the duration of TGF source is predominantly greater than the time dispersion induced by Compton scattering.

The results of present work show that the rise and fall times of Fermi-measured TGFs (Foley et al., 2014) can be fully explained using TGF sources with a Gaussian-shaped temporal distribution and characteristic durations between 80 and 1,000 μs, without any further model-specific assumptions (see Figure 3). We have also tested that a duration of 50 μs should be among the shortest sources that are consistent with Fermi measurements. This range of source duration is in line with both the timescale of negative corona flashes during IC discharges (Moss et al., 2006) and the relativistic feedback discharges (Dwyer, 2012). The duration of negative corona flashes is determined by the speed of streamers and the eventual size of the streamer zone formed

in front of lightning leaders (Moss et al., 2006). Typical values for the duration of negative corona flashes associated with high-potential lightning leaders in +ICs are between a few tens of microseconds and a fraction of milliseconds (e.g., Moss et al., 2006; Xu et al., 2015). The duration of relativistic feedback discharge can range from tens of microseconds up to ∼1 ms, depending on the relativistic feedback factor (Dwyer, 2012). In this regard, the rise and fall times of Fermi-measured TGFs solely are insufficient to distinguish one process from the other.

This study is a theoretical work with the aim toward better understanding of Compton scattering effects and tilted TGF geometry, and instrumental limitations are not considered in the comparison with Foley et al. (2014). Nevertheless, the instrumental effects, for example, dead time and pulse pileup, on the temporal parameters of TGF pulses have been found to be marginal (Foley et al., 2014; Tierney et al., 2013). As noted by Tierney et al. (2013), "the major effects of applying the dead-time correction were on the maximum rate and total counts of the TGF pulse. Other temporal parameters such as the full width at half maximum (FWHM) and rise/fall times were not significantly affected." To examine these effects, Foley et al. (2014) performed detailed Monte Carlo simulations and revealed that these effects are generally small on temporal parameters and the influence is mostly on the fall time of asymmetric pulses, with a maximum elongation of fall time by 20–30 μs for very asymmetric pulses. It is conceivable that instrumental effects could influence our simulation results presented in Figure 3c but mainly the temporal space above the unity line around the rise time of ∼20 μs and fall time of ∼100 μs as produced by the source duration of 80 μs. The fall times in this region could be shifted upward by 20–30 μs, and in this case, the agreement with the analysis of Foley et al. (2014) would become even better.

The energy distributions and light curves presented in Figures 1c and 1d are clear indications that offset distance between the lightning source and satellite location is not a robust measure of Compton scattering effects. The source orientation is a critical parameter in TGF analysis but has been significantly underestimated in previous studies. The extent of Compton scattering in both tilted and untilted geometry is roughly proportional to the distance between where the source beam is pointed at and where photons are recorded. At locations outside the source photon beam, as this distance increases, the corresponding energy distribution softens, and the light curve becomes accordingly flatter. Inside this beam, the light curve receives less contribution from Compton-scattered photons, and the energy distribution generally exhibits the typical high-energy cutoff. Depending on how tilted the TGF source is, the increase in t_{50} could be as large as ∼9 and ∼66 μs for the rising and falling parts, respectively. Furthermore, TGFs are believed to be produced by initial leaders during the development stage of IC discharges (e.g., Lyu & Cummer, 2018; Marshall et al., 2013), and the initial leaders are almost certainly tilted during some steps. As such, taking the tilted geometry into account would be imperative for future studies aiming to unbiasedly investigate TGF sources.

With both satellite and radio measurements, present results may provide a means to infer if and how the TGF-producing process is tilted. For example, if photons recorded at a close offset distance are atypically less energetic with an anomalously long pulse duration, it is probable that the TGF source is not pointed toward the satellite location. Comparing satellite and/or radio measurements with present results can thus help filter out the Compton scattering effects, thereby better constraining the properties of TGF source. Moreover, both the Atmosphere-Space Interaction Monitor mission (ASIM) (Neubert et al., 2019) and the Tool for the Analysis of RAdiation from lightNIng and Sprites (TARANIS) (Lefeuvre et al., 2008) are equipped with photometric and particle detectors to locate TGFs and the lightning source. Therefore, present results are also of timely importance in view of the scientific goals of these ongoing and upcoming space missions.

5. Conclusions

The main contributions of this work can be summarized as follows:

1. Using a Monte Carlo model, we have simulated the light curve and energy spectra of TGFs in both tilted and vertical source geometry. Specifically, we have investigated the effects of Compton scattering on the symmetry properties and rise and fall times in the vertical source geometry and on the temporal and spectral properties of TGFs in the tilted source geometry.
2. We have explained the symmetric and asymmetric TGF pulses measured by Fermi GBM, as well as their rise and fall time distributions. These TGF pulses are found to be consistent with TGF sources with a Gaussian temporal distribution and an average duration of ∼206 μs in the context of Compton scattering

effects. Nevertheless, we note that these pulses provide inadequate information to distinguish the two main mechanisms that have been so far proposed for TGFs (Celestin & Pasko, 2011; Dwyer, 2008; 2012).

3. We show that the effects of Compton scattering are mainly carried by the ensemble of relatively low-energy photons, for example, with energies less than 500 keV. The extent of Compton scattering effects can be roughly evaluated using the distance between where the source photon beam is pointed at and where photons are recorded. If measured outside the source photon beam, the effects of Compton scattering would be enhanced with increasing tilt angle, leading to softer energy spectra and flatter light curves. Furthermore, we have quantified the effects of Compton scattering on both the rising and falling parts of TGF light curves in terms of increase in t_{50}. Together with coordinated satellite and radio measurements, these results may be used to determine the orientation of TGF sources.
4. The tilted source geometry causes asymmetry in the population of photons that escape the atmosphere with respect to the zenith direction. We therefore suggest that offset distance between the lightning source and satellite location cannot be used as a single parameter to characterize Compton scattering effects. Moreover, our results emphasize the need to take the tilted source geometry into account while analyzing satellite measurements, for example, with the aid of interferometric observation of initial leader steps.

Acknowledgments
This research was supported by the NSF Grants AGS-1243176 and AGS-1732359. Sebastien Celestin's work was supported by the French space agency (CNES) in the framework of the satellite project TARANIS. The simulation data and analysis codes used to generate all figures and results in this paper are available online (https://github.com/wexu6668/compton_2019).

References

Briggs, M. S., Fishman, G. J., Connaughton, V., Bhat, P. N., Paciesas, W. S., Preece, R. D., et al. (2010). First results on terrestrial gamma ray flashes from the Fermi Gamma-ray Burst Monitor. *Journal of Geophysical Research*, *115*, A07323. https://doi.org/10.1029/2009JA015242

Briggs, M. S., Xiong, S., Connaughton, V., Tierney, D., Fitzpatrick, G., Foley, S., et al. (2013). Terrestrial gamma-ray flashes in the Fermi era: Improved observations and analysis methods. *Journal of Geophysical Research: Space Physics*, *118*, 3805–3830. https://doi.org/10.1002/jgra.50205

Carlson, B. E., Lehtinen, N. G., & Inan, U. S. (2007). Constraints on terrestrial gamma ray flash production from satellite observation. *Geophysical Research Letters*, *34*, L08809. https://doi.org/10.1029/2006GL029229

Celestin, S., & Pasko, V. P. (2011). Energy and fluxes of thermal runaway electrons produced by exponential growth of streamers during the stepping of lightning leaders and in transient luminous events. *Journal of Geophysical Research*, *116*, A03315. https://doi.org/10.1029/2010JA016260

Celestin, S., & Pasko, V. P. (2012). Compton scattering effects on the duration of terrestrial gamma-ray flashes. *Geophysical Research Letters*, *39*, L02802. https://doi.org/10.1029/2011GL050342

Celestin, S., Xu, W., & Pasko, V. P. (2012). Terrestrial gamma ray flashes with energies up to 100 MeV produced by nonequilibrium acceleration of electrons in lightning. *Journal of Geophysical Research*, *117*, A05315. https://doi.org/10.1029/2012JA017535

Celestin, S., Xu, W., & Pasko, V. P. (2015). Variability in fluence and spectrum of high-energy photon bursts produced by lightning leaders. *Journal of Geophysical Research: Space Physics*, *120*, 10,712–10,723. https://doi.org/10.1002/2015JA021410

Connaughton, V., Briggs, M. S., Holzworth, R. H., Hutchins, M. L., Fishman, G. J., Wilson-Hodge, C. A., et al. (2010). Associations between Fermi Gamma-ray Burst Monitor terrestrial gamma ray flashes and sferics from the World Wide Lightning Location Network. *Journal of Geophysical Research*, *115*, A12307. https://doi.org/10.1029/2010JA015681

Connaughton, V., Briggs, M. S., Xiong, S., Dwyer, J. R., Hutchins, M. L., Grove, J. E., et al. (2013). Radio signals from electron beams in terrestrial gamma ray flashes. *Journal of Geophysical Research: Space Physics*, *118*, 2313–2320. https://doi.org/10.1029/2012JA018288

Cummer, S. A., Briggs, M. S., Dwyer, J. R., Xiong, S., Connaughton, V., Fishman, G. J., et al. (2014). The source altitude, electric current, and intrinsic brightness of terrestrial gamma ray flashes. *Geophysical Research Letters*, *41*, 8586–8593. https://doi.org/10.1002/2014GL062196

Dwyer, J. R. (2008). Source mechanisms of terrestrial gamma-ray flashes. *Journal of Geophysical Research*, *113*, D10103. https://doi.org/10.1029/2007JD009248

Dwyer, J. R. (2012). The relativistic feedback discharge model of terrestrial gamma ray flashes. *Journal of Geophysical Research*, *117*, A02308. https://doi.org/10.1029/2011JA017160

Dwyer, J. R., & Smith, D. M. (2005). A comparison between Monte carlo simulations of runaway breakdown and terrestrial gamma-ray flash observations. *Geophysical Research Letters*, *32*, L22804. https://doi.org/10.1029/2005GL023848

Dwyer, J. R., Smith, D. M., & Cummer, S. A. (2012). High-energy atmospheric physics: Terrestrial gamma-ray flashes and related phenomena. *Space Science Reviews*, *173*, 133–196. https://doi.org/10.1007/s11214-012-9894-0

Fishman, G. J., Bhat, P. N., Mallozzi, R., Horack, J. M., Koshut, T., Kouveliotou, C., et al. (1994). Discovery of intense gamma-ray flashes of atmospheric origin. *Science*, *264*(5163), 1313–1316.

Fishman, G. J., Briggs, M. S., Connaughton, V., Bhat, P. N., Paciesas, W. S., von Kienlin, A., et al. (2011). Temporal properties of the terrestrial gamma-ray flashes from the Gamma-Ray Burst Monitor on the Fermi Observatory. *Journal of Geophysical Research*, *116*, A07304. https://doi.org/10.1029/2010JA016084

Fitzpatrick, G., Cramer, E., McBreen, S., Briggs, M. S., Foley, S., Tierney, D., et al. (2014). Compton scattering in terrestrial gamma-ray flashes detected with the Fermi gamma-ray burst monitor. *Physical Review D*, *90*(4), 43008.

Foley, S., Briggs, M. S., Connaughton, V., Tierney, D., McBreen, S., Dwyer, J. R., et al. (2014). Pulse properties of terrestrial gamma-ray flashes detected by the Fermi Gamma-Ray Burst Monitor. *Journal of Geophysical Research: Space Physics*, *119*, 5931–5942. https://doi.org/10.1002/2014JA019805

Gjesteland, T., Østgaard, N., Connell, P. H., Stadsnes, J., & Fishman, G. J. (2010). Effects of dead time losses on terrestrial gamma ray flash measurements with the Burst and Transient Source Experiment. *Journal of Geophysical Research*, *115*, A00E21. https://doi.org/10.1029/2009JA014578

Grefenstette, B. W., Smith, D. M., Dwyer, J. R., & Fishman, G. J. (2008). Time evolution of terrestrial gamma ray flashes. *Geophysical Research Letters*, *35*, L06802. https://doi.org/10.1029/2007GL032922

Hazelton, B. J., Grefenstette, B. W., Smith, D. M., Dwyer, J. R., Shao, X.-M., Cummer, S. A., et al. (2009). Spectral dependence of terrestrial gamma-ray flashes on source distance. *Geophysical Research Letters*, *36*, L01108. https://doi.org/10.1029/2008GL035906

Lefeuvre, F., Blanc, E., Pinçon, J.-L., Roussel-Dupré, R., Lawrence, D., Sauvaud, J.-A., et al. (2008). TARANIS—A satellite project dedicated to the physics of TLEs and TGFs. *Space Science Reviews*, *137*, 301–315.

Lu, G., Blakeslee, R. J., Li, J., Smith, D. M., Shao, X.-M., McCaul, E. W., et al. (2010). Lightning mapping observation of a terrestrial gamma-ray flash. *Geophysical Research Letters*, *37*, L11806. https://doi.org/10.1029/2010GL043494

Lyu, F., & Cummer, S. A. (2018). Energetic radio emissions and possible terrestrial gamma-ray flashes associated with downward propagating negative leaders. *Geophysical Research Letters*, *45*, 10,764–10,771. https://doi.org/10.1029/2018GL079424

Lyu, F., Cummer, S. A., Lu, G., Zhou, X., & Weinert, J. (2016). Imaging lightning intracloud initial stepped leaders by low-frequency interferometric lightning mapping array. *Geophysical Research Letters*, *43*, 5516–5523. https://doi.org/10.1002/2016GL069267

Mailyan, B. G., Briggs, M. S., Cramer, E. S., Fitzpatrick, G., Roberts, O. J., Stanbro, M., et al. (2016). The spectroscopy of individual terrestrial gamma-ray flashes: Constraining the source properties. *Journal of Geophysical Research: Space Physics*, *121*, 11,346–11,363. https://doi.org/10.1002/2016JA022702

Mailyan, B. G., Nag, A., Murphy, M. J., Briggs, M. S., Dwyer, J. R., Rison, W., et al. (2018). Characteristics of radio emissions associated with terrestrial gamma-ray flashes. *Journal of Geophysical Research: Space Physics*, *123*, 5933–5948. https://doi.org/10.1029/2018JA025450

Marisaldi, M., Fuschino, F., Labanti, C., Galli, M., Longo, F., Del Monte, E., et al. (2010). Detection of terrestrial gamma ray flashes up to 40 MeV by the AGILE satellite. *Journal of Geophysical Research*, *115*, A00E13. https://doi.org/10.1029/2009JA014502

Marshall, R. A., da Silva, C. L., & Pasko, V. P. (2015). Elve doublets and compact intracloud discharges. *Geophysical Research Letters*, *42*, 6112–6119. https://doi.org/10.1002/2015GL064862

Marshall, T., Stolzenburg, M., Karunarathne, S., Cummer, S., Lu, G., Betz, H.-D., et al. (2013). Initial breakdown pulses in intracloud lightning flashes and their relation to terrestrial gamma ray flashes. *Journal of Geophysical Research: Atmospheres*, *118*, 10,907–10,925. https://doi.org/10.1002/jgrd.50866

Moss, G. D., Pasko, V. P., Liu, N., & Veronis, G. (2006). Monte Carlo model for analysis of thermal runaway electrons in streamer tips in transient luminous events and streamer zones of lightning leaders. *Journal of Geophysical Research*, *111*, A02307. https://doi.org/10.1029/2005JA011350

Nemiroff, R. J., Bonnell, J. T., & Norris, J. P. (1997). Temporal and spectral characteristics of terrestrial gamma flashes. *Journal of Geophysical Research*, *102*(A5), 9659–9666. https://doi.org/10.1029/96JA03107

Neubert, T., Østgaard, N., Reglero, V., Blanc, E., Chanrion, O., Oxborrow, C. A., et al. (2019). The ASIM Mission on the International Space Station. *Space Science Reviews*, *215*, 26.

Norris, J. P., Nemiroff, R. J., Bonnell, J. T., Scargle, J. D., Kouveliotou, C., Paciesas, W. S., et al. (1996). Attributes of pulses in long bright gamma-ray bursts. *The Astrophysical Journal*, *4549*, 393–412. https://doi.org/10.1086/176902

Østgaard, N., Gjesteland, T., Hansen, R. S., Collier, A. B., & Carlson, B. (2012). The true fluence distribution of terrestrial gamma flashes at satellite altitude. *Journal of Geophysical Research*, *117*, A03327. https://doi.org/10.1029/2011JA017365

Østgaard, N., Gjesteland, T., Stadsnes, J., Connell, P. H., & Carlson, B. (2008). Production altitude and time delays of the terrestrial gamma flashes: Revisiting the Burst and Transient Source Experiment spectra. *Journal of Geophysical Research*, *113*, A02307. https://doi.org/10.1029/2007JA012618

Roberts, O. J., Fitzpatrick, G., Stanbro, M., McBreen, S., Briggs, M. S., Holzworth, R. H., et al. (2018). The First Fermi-GBM Terrestrial Gamma Ray Flash Catalog. *Journal of Geophysical Research: Space Physics*, *123*, 4381–4401. https://doi.org/10.1029/2017JA024837

Shao, X.-M., Hamlin, T., & Smith, D. M. (2010). A closer examination of terrestrial gamma-ray flash-related lightning processes. *Journal of Geophysical Research*, *115*, A00E30. https://doi.org/10.1029/2009JA014835

Smith, D. M., Lopez, L. I., Lin, R. P., & Barrington-Leigh, C. P. (2005). Terrestrial gamma-ray flashes observed up to 20 MeV. *Science*, *307*(5712), 1085–1088.

Stanley, M. A., Shao, X.-M., Smith, D. M., Lopez, L. I., Pongratz, M. B., Harlin, J. D., et al. (2006). A link between terrestrial gamma-ray flashes and intracloud lightning discharges. *Geophysical Research Letters*, *33*, L06803. https://doi.org/10.1029/2005GL025537

Tierney, D., Briggs, M. S., Fitzpatrick, G., Chaplin, V. L., Foley, S., McBreen, S., et al. (2013). Fluence distribution of terrestrial gamma ray flashes observed by the Fermi Gamma-ray Burst Monitor. *Journal of Geophysical Research: Space Physics*, *118*, 6644–6650. https://doi.org/10.1002/jgra.50580

Xu, W., Celestin, S., & Pasko, V. P. (2012). Source altitudes of terrestrial gamma-ray flashes produced by lightning leaders. *Geophysical Research Letters*, *39*, L08801. https://doi.org/10.1029/2012GL051351

Xu, W., Celestin, S., & Pasko, V. P. (2014). Modeling of X-ray emissions produced by stepping lightning leaders. *Geophysical Research Letters*, *41*, 7406–7412. https://doi.org/10.1002/2014GL061163

Xu, W., Celestin, S., & Pasko, V. P. (2015). Optical emissions associated with terrestrial gamma ray flashes. *Journal of Geophysical Research: Space Physics*, *120*, 1355–1370. https://doi.org/10.1002/2014JA020425

Xu, W., Celestin, S., Pasko, V. P., & Marshall, R. A. (2017). A novel type of transient luminous event produced by terrestrial gamma-ray flashes. *Geophysical Research Letters*, *44*, 2571–2578. https://doi.org/10.1002/2016GL072400